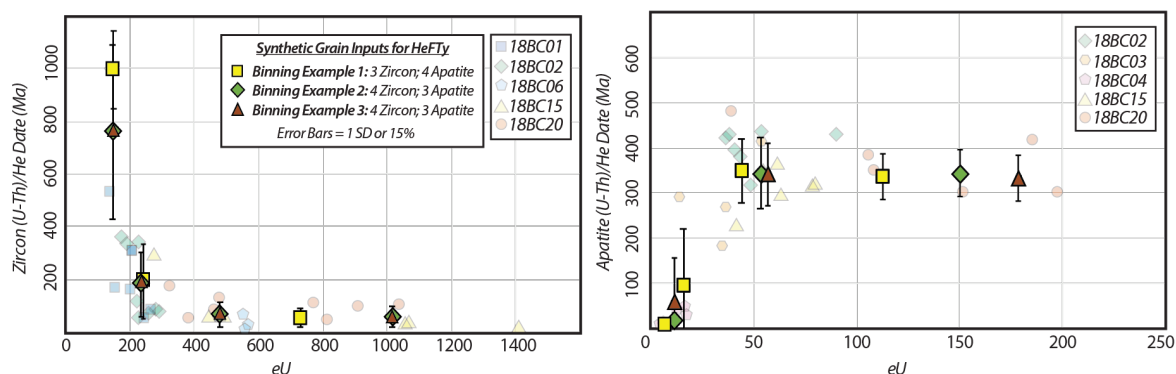
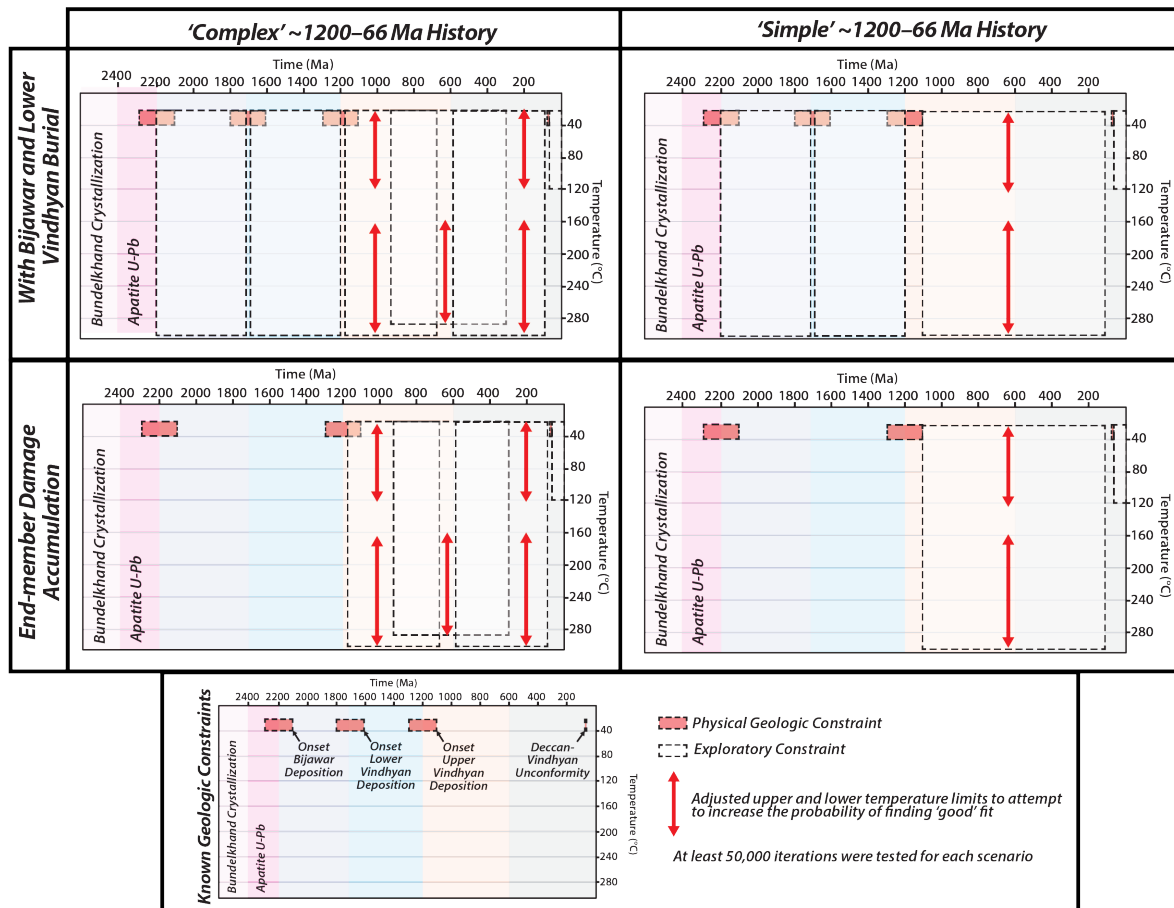


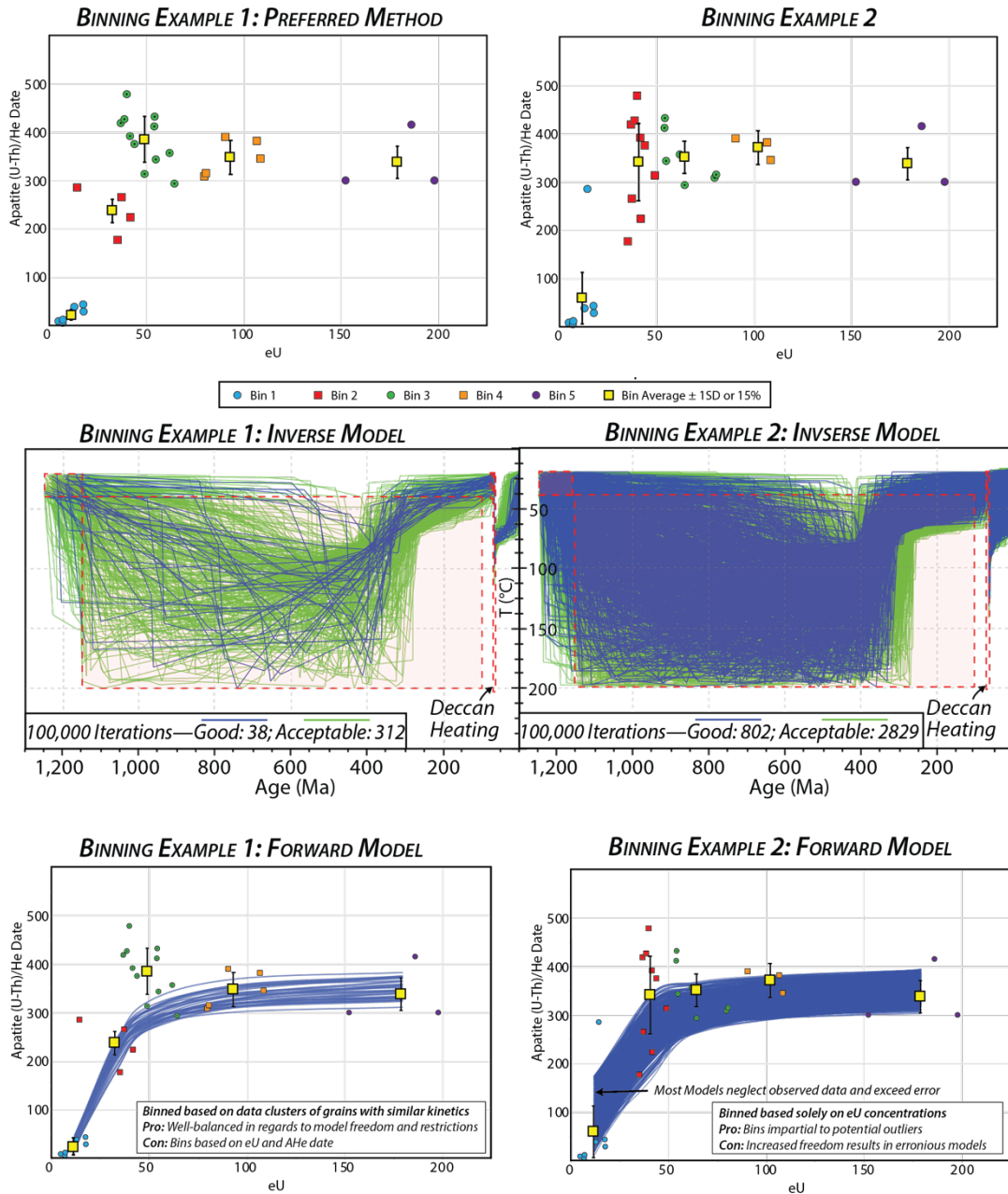
### BINNING EXAMPLES FROM EASTERN CRATON MARGIN



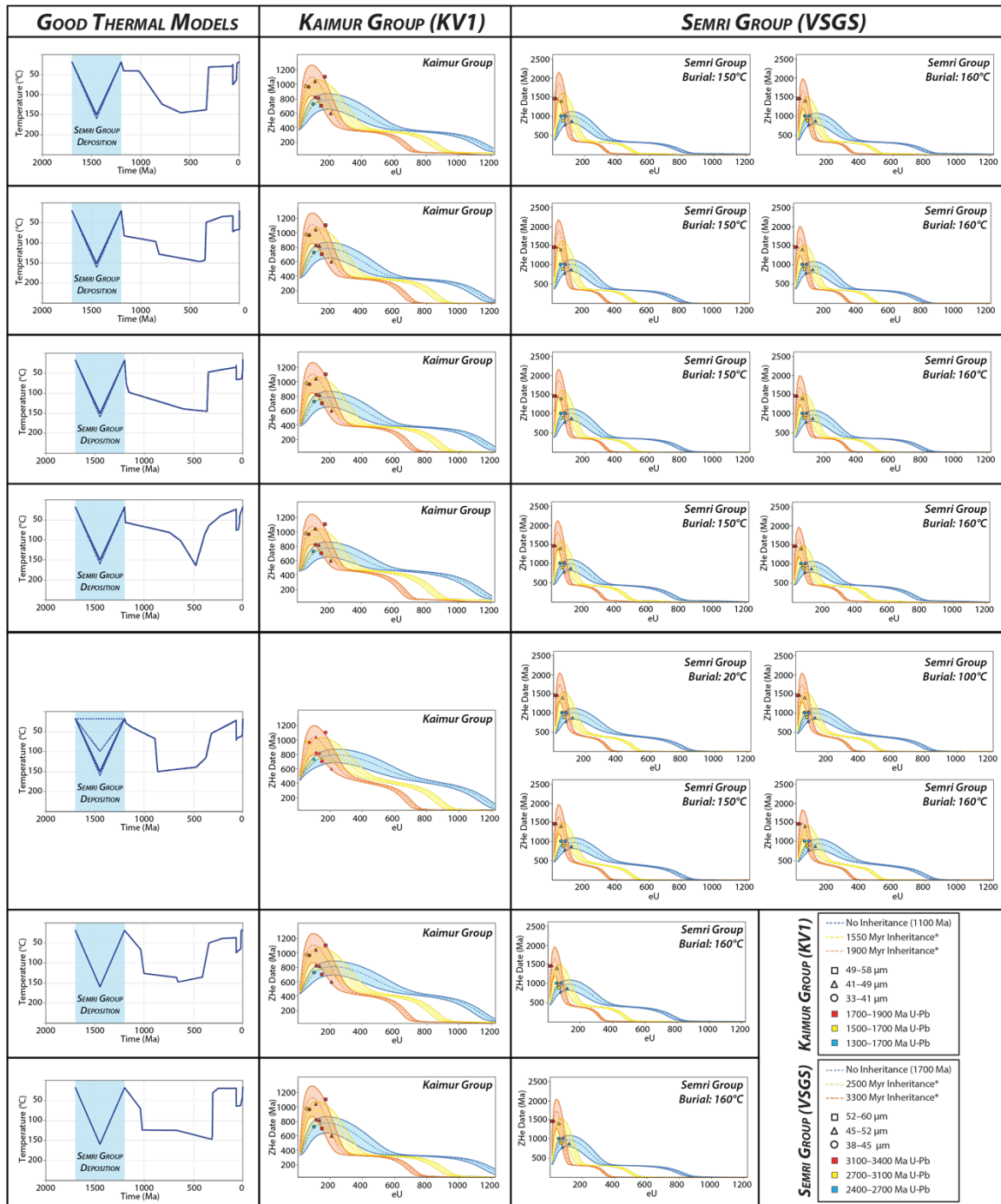
**Supplementary Figure 1:** Example from the eastern craton margin of various strategies utilized to ‘bin’ the couple ZHe and AHe data into synthetic grain inputs for inverse modelling in HeFTy. As HeFTy permits the input of 7 datapoints, the coupled ZHe and AHe datasets were separated into bins defined by eU concentrations that best represent the date-eU relationship for each system. Differing combinations of ZHe and AHe bins were tested, and the combinations above represent only select examples. Synthetic grain inputs include the average grain size, uncorrected date, and U-Th-Sm concentrations of the single-grain data within each defined bin, and ZRDAAM and RDAAM parameters were selected for zircon and apatite inputs, respectively. For each synthetic data input, an error of 1 standard deviation or 15% was utilized (whichever was greater). Similar binning approaches were also tested using AHe and ZHe data from the central, northeastern, and western craton compilations.



**Supplementary Figure 2:** Examples of known geological and exploratory constraints utilized in HeFTy for inverse models using the couple AHe and ZHe datasets. Various scenarios were tested to permit the model to explore a ‘complex’ and ‘simple’ ~1200–66 Ma history, where much of the geological history remains uncertain. The ‘complex’ scenario permits two phases of heating and cooling following Upper Vindhyan burial, whereas the ‘simple’ scenario permits a single phase of heating and cooling. Red vertical arrows indicate that the upper and lower limits of the temperature constraints were systematically restricted in an attempt to increase the probability of finding ‘acceptable’ and ‘good’ pathways—models with too much freedom may prevent finding fits to the data. In many cases, maximum burial constraints from ~1200–66 Ma was adjusted to below ~180 °C based on the abundance of detrital ZHe dates exceeding 1.0 Ga. End-member thermal inversions were also tested, which forced the extreme accumulation of radiation damage from ~2.2 Ga to 1.2 Ga. In each tested inverse model (with various synthetic grain inputs), no ‘good’ thermal history resulted after running at least 50,000 iterations (many tests included >1,000,000 iterations). In rare cases, ~1-2 “acceptable” pathways resulted per ~100,000 iterations. We note that the scarcity of these histories hinders reliable interpretations. Furthermore, forward models from these rare ‘acceptable’ pathways reveal that the model predictions still significantly deviate from the majority of observed data.



**Supplementary Figure 3:** Summary of inverse model set-up and results using only AHe data from the eastern craton margin (from Colleps et al., 2021a). Two differing binning strategies are shown to illustrate model sensitivities to how synthetic grain inputs are defined. Example one bins data based on statistically defined clusters of data, in which we assume reflect clusters of data with similar kinetic behavior. Example two bins strictly based on eU concentrations. Both examples avoid the exclusion of non-obvious outliers, such as a  $\sim$ 285 Ma grain with an eU concentration of 15 ppm which follows the general date-eU relationship. However, the inclusion of this data point in the low eU bin of example 2 induces a large error on the synthetic grain input. Consequently, using this binning approach provides the model with too much freedom, and more than half of the ‘good’ fit pathways neglect the majority of observed data. We argue that binning example 1 provides a balance of model freedom and restrictions, and we use this binning approach to generate 500 ‘good’ time-temperature pathways for detrital zircon inheritance envelope date-eU forward models. For complete discussion on AHe thermal inversions and model sensitivities to various parameters (binning, bounding constraints, etc.) we refer the reader to Colleps et al. (2021a).



**Supplementary Figure 4:** Detrital ZHe date-eU inheritance envelopes for all 14 t-T pathways denoted with “good” fit, revealing how forward models agree with observed ZHe data from the Vindhyan deposits. Of the 14 pathways, 7 t-T pathways yield identical thermal histories from ~1.2 Ga to the present with variable degrees of heating during deposition of the Lower Vindhyan Semri Group.